

ISSN Online 2617-3573



Development of an Automated Hall Effect Experimentation Method for the Electrical Characterization of Thin Films

A. Orega, M. Mwamburi & C. Maghanga

ISSN: 2617-3573

Development of an Automated Hall Effect Experimentation Method for the Electrical Characterization of Thin Films

^{*1}A.Orega

Kabarak University, Kenya, Department of Physical Sciences and Biological Sciences

*Email of corresponding authors: al.for@live.com

²M. Mwamburi

University of Eldoret, Department of Physics

³C. Maghanga

Kabarak University, Kenya, Department of Physics and Biological Sciences

How to cite this article: Orega, A., Mwamburi, M. & Maghanga, C. (2023). Development of an Automated Hall Effect Experimentation Method for the Electrical Characterization of Thin Films. *Journal of Information and Technology*, 7(1), 58-68. <https://doi.org/10.53819/81018102t4208>

Abstract

There has been drastic growth in the microelectronics industry in the recent past. The performance of these materials is influenced by their structural, electrical, and optical properties among others, depending on their applications. Therefore, the need to conduct measurements of the semiconductor characteristics precisely, quickly, and conveniently cannot be overstated. Some of the desirable features of measurements include usability, accuracy, resolution, repeatability, and consistency which cannot be assured with manually operated systems. This study strived to design and interface an automated computer-aided four-point probe test equipment that characterizes materials to determine their electrical properties. A four-point probe head, an electromagnet, NI Keithley model 6220 Precision current source, model 7001 switch, model 2182A Nanovoltmeter, and model 7065 Hall Effect card instruments were interfaced with the NI LabVIEW program running in a computer through a GPIB hub to a PC USB for its full control. The four-probe head was utilized to probe the samples with a square symmetry that was adopted for the measurement of the semiconductor properties. Reliability tests were conducted on a standard P-type Germanium sample. The collected data was within 0.32% of the expected results. This work forms a basis for automating similar systems that were inherently designed to be operated manually.

Keywords: *Automated Hall Effect, manually operated systems, Hall angle, thin films, string manipulation routines.*

1.0 Introduction

Thin-film semiconductors have recently attracted a lot of attention because of their scientific and technological importance^[1]. Demand for semiconductors is expected to rise significantly in the coming years as chips become even more deeply embedded in the current and upcoming technologies^[2], which aligns with the prediction of Moore's law^[3].

Thin-film characterization has relentlessly advanced over time to improve materials assessment quality and reliability. This comprises physical, chemical, optical, and electrical characterization. Rapid advances in the efficiency and production of materials including semiconductors have been vital factors of technological dominance^[4]. Materials with sophisticated electrical characteristics are in high demand for the production of a wide range of information technology products^[5]. In electrical characterization, physical parameters such as resistivity, conductivity, charge carrier concentration, and mobility, as well as charge carriers' type - electrons or holes, are of significant interest and can be determined by measuring the Hall effect^[6, 7], which is among the most important semiconductor characterization techniques^[8] used in both industries and research.

In electrical characterization, the four-point probe technique has evolved into an integrative characterization tool in various disciplines and fields, and it is used for both profound and application-driven studies^[9]. The technique involves determining a material's electrical properties by passing a small current through two contacts and measuring the potential difference between the two of them.

The Hall effect is a physical phenomenon that occurs in certain materials when they are placed in a magnetic field^[10]. When a magnetic field is applied perpendicular to the direction of an electric current flowing through the material, the electrons in the material will be deflected, resulting in a measurable voltage across the material that is perpendicular to both the magnetic field and the current direction. This effect can be used to measure the strength of magnetic fields, the concentration of charge carriers in a material, and the mobility of these charge carriers. The Hall effect has numerous applications in various fields such as electronics, materials science, and physics^[6].

The development in technology and computer literacy among users, as well as the growing popularity of Internet connection, has provided various institutions around the world with an opportunity to enhance outcomes and provide access to a larger number of students^[11]. Similarly, technology is used as a tool to conduct laboratory research. This technology can range from a simple manual data recorder in the form of a spreadsheet^[12] to a very sophisticated experimentation system in which the computer controls the entire setup, providing a laboratory experience by making simulation programs of laboratory exercises via computer programs^[13] or having a remote laboratory which is equipped with real instruments, allowing for experiments to be carried out by operating the devices and viewing real data from a distant place via the network^[14].

2.1 Theoretical Review

Traditional electrical characterization of materials is often plagued with inefficiencies and inaccuracies arising from human factors owing to the immense data that must be manually acquired and analyzed. These can be minimized by automation which may provide several advantages, such as improved speed, accuracy, and error reduction as evidenced by the works of Agumba *et al*^[15], Cervantes *et al*^[16], Garnica *et al*^[17], and Valladares *et al*^[18]. However, their systems were limited to obtaining thin-film sheet resistivity, conductivity, capacitance measurements since they are based on I-V and temperature measurements as shown in Table 1 below and did not support remote experimentation.

Table 1: Summary of Previous Related Research and their Limitations

Research	Key Output	Limitation
Design And Fabrication of a Simple Four Point Probe System for Electrical Characterization of Thin Films. Agumba <i>et al</i> ^[15]	Developed a computer-aided four-point probe system for measuring thin film sheet resistivity	It was limited to resistivity measurements. Accuracy was lowered due to the induced Schottky effect by the aluminium probe tips used.
Development and Automation of a Thermoelectric Characterization System. Cervantes <i>et al</i> ^[16]	Developed an automated thermoelectric characterization system	It was limited to resistivity and conductivity measurements at various temperatures.
Automatic Micro-Robotic Identification and Electrical Characterization of Graphene. Garnica <i>et al</i> ^[17]	Automated a procedure to identify graphene flakes electrically and characterize them	It was limited to conductivity measurements.
Design and Implementation of an Automatic System for Dielectric Characterization of Ceramic Materials. Valladares <i>et al</i> ^[18]	Designed an automatic characterization system to calculate the complex impedance and dielectric constant at various temperatures.	It was limited to capacitance and conductance measurements.

This paper reports on a system that is not limited to conducting thin-film sheet resistivity, conductivity and capacitance measurements but is able to additionally obtain the Hall voltage, charge carrier mobility, carrier concentration, Hall coefficient, Hall angle and the conductivity type (N or P) of thin-film sheets which cannot be obtained by ordinary four-point probe I-V measurements.

3.0 Device Setup and Configuration

Dedicated instruments were used to collect the data which was then stored and analyzed using a computer program to obtain the electric properties of a germanium sample. The whole process of data acquisition and analysis was automated by the use of the following instruments and software.

- i. Keithley 6220 Precision current source
- ii. Keithley 2182A Nanovoltmeter
- iii. Keithley 7001 Switch
- iv. Model 7065 Hall Effect card
- v. 258.125mT Fixed Magnet
- vi. LabVIEW IDE

A fabricated four-point probe was used to hold the semiconductor sample. Consisting of two soft cores, this was used to generate the magnetic field required for the experiment. A dedicated computer was used to precisely measure the magnitude of the magnetic field produced.

The Keithley measurement instruments and the PC were communicated interchangeably using USB and GPIB protocols. Copper wires were used in closing the circuits. The Four-point probe, the PC, and the Keithley instruments were interconnected

Probes A and C were connected to the precise current source while probes B and D were connected to Model 2182A as depicted in Figure 1 and 2. The current source provided current to the outer two probes, while the voltmeter was used to measure the voltage between the inner two probes. The Probed sample was then placed perpendicularly to a magnetic field provided by the electromagnets.

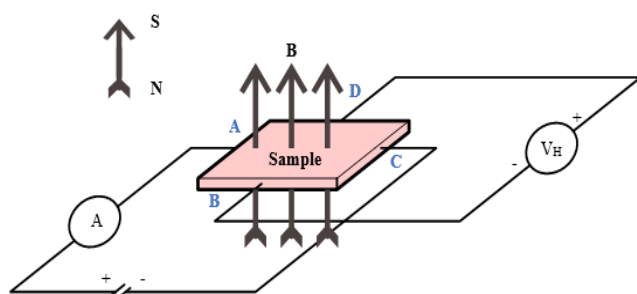


Figure 1: Probing on a four-point probe holder with a rectangular shaped sample

A USB port, USB to GPIB cables, and a GPIB Hub were used to connect the instruments to the PC. As a standard tool for creating interfaces, NI-VISA enables the configuration, programming, and debugging of instruments and equipment as well as the acquisition of data from external sensors using any type of communication port, including Ethernet, GPIB, USB, and others^[19]. The 7001 switch employs cards that can accommodate a wide range of signals while maintaining high accuracy and signal quality. These cards reduce signal errors and protect against signal degradation caused by offset voltage, isolation resistance, and leakage current. 7065 low current scanner card model: an 8-channel, 2-pole card with a thermal offset of 30nV. In the card 1 slot of the 7001-switch system, a 25-channel pA-Multiplexer with BNC socket was installed. The test sample was connected to channel two of the multiplexer card and the 6220 Current source output was connected to channel one as shown in Figure 2.

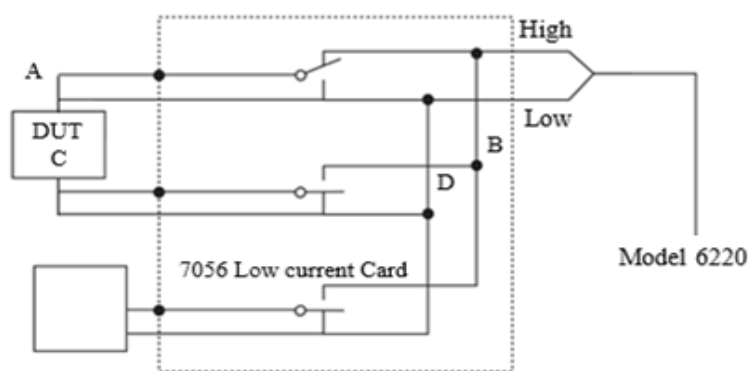


Figure 2: Test Sample

Model 7065 Hall Effect card facilitated switching digital output using assigned channels by model 7001. LabVIEW a full-featured programming language with a variety of data types, loops, data structures, conditional statements, string manipulation routines, arrays, and file Input/output methods, among other things^[20] was used. Hence floating-point numeric data types with double precision and associated physical quantities of the measure were used for

both data collection and input while string data types were used for output statements like simple text messages. LabVIEW-based VIs and sub-VIs coupled with SCPI commands were used for both data input and collection from the Instruments. Instruments data was observed, collated, evaluated, and analyzed within the LabVIEW software. The obtained was exported as a CSV file giving an option of transferring to spreadsheets or any other application for further manipulations.

The Model 2182A and the ammeter readings were collected remotely from the Keithley instruments by coded data acquisition VIs via the NI-VISA architecture and SCPI commands. The NI-VISA facilitated the communication between the Keithley instruments and the PC while LabVIEW acted as the system controller operating all the devices simultaneously^[21]. A test report was initially obtained and commenced by ensuing empirical data collection. Using the obtained data, the electrical properties were automatically computed using the coded Sub-VIs. To obtain precise and accurate information, the program iterated using execution structures by conducting a sweep in the DC source with the option of repeating the procedure at several defined times and intervals.

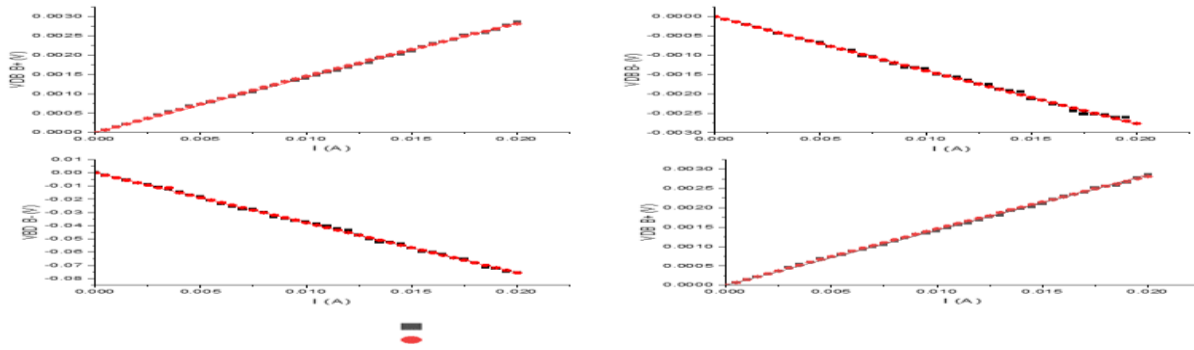
The data collected was stored in arrays then the average resistance followed by other parameters was calculated. The procedure continued until parameters within the user-defined range are obtained. Then the program stops, records, and analyzes the values obtained.

Data was collected and recorded at increasing current thrice in predefined steps to check on the systems' consistency and repeatability. The first set of data was used to develop a mathematical model that connects the input data and the desired data while the second set was used to test the validity of the models. For valid data, the second part percentage error should not differ by more than a little amount, such as 2 or 3 per cent according to Yousif^[22].

A wide range of data points was collected to minimize the effect of individual measurement errors. For error analysis, random errors were collected from the instruments' precision and the experiment was repeatedly done to check for systematic errors. The data automatically recorded for the available Germanium sample were tabulated and compared with manually done experimental values. The LabVIEW software used the least square regression analysis from the $V - I$ data recorded to determine the resistance of the sample and thereafter calculated the other parameters.

4.0 Results and Discussions

VI graphs for the above data were drawn alongside the data obtained automatically by the LabVIEW application and analyzed using the OriginPro application package. The graphs are collated in Figure 3.



Manually obtained data

Figure 3: Manually obtained vs automatically obtained VI Data Graphs

The line of best fit was drawn using the least square method. The analysis was derived afterward and is presented in Table 2.

Table 2: Manually obtained VI data analysis

Plot	Weight	Intercept	Slope	Residual Sum of Squares	Pearson's r	R-Square (COD)	Adj. R-Square
VBD	No	0 ± --	3.82505 ±	2.71E-05	0.99983	0.99967	0.99966
B+	Weighting		0.01106				
VDB	No	0 ± --	-0.13896 ±	5.64546E-8	-0.9997	0.99947	0.99946
B-	Weighting		5.04965E-4				
VBD	No	0 ± --	-3.7776 ±	2.5837E-5	-0.9998	0.99967	0.99966
B-	Weighting		0.0108				
VDB	No	0 ± --	0.1418 ±	9.54E-08	0.99957	0.99914	0.99912
B+	Weighting		6.56255E-4				

When the experiment is conducted manually and contrast drawn between the variables, the following data presented in Table 3 were obtained.

Table 3: Comparison between Automated and Manually Obtained Values

Quantity	Automated	Manual	Error (%)
Resistivity (mΩm)	3.954216	3.941706	0.32
Conductivity (S/m)	252.894632	253.697257	0.32
Hall Co-efficient (mOhm m/T)	7.659498305	7.63526586	0.32
Carrier Mobility (/T)	1.937046005	1.937046005	0.00
Hall Angle (rad)	0.46365	0.46364	0.00
Charge Carrier Concentration (/m ³)	8.14872E+20	8.17458E+20	0.32
Resistance (Ω)	1.97711	1.97085	0.32

At a room temperature of 292.45 K, the Coefficient was measured to be 7.6595 mΩm/T, and the carrier concentration was measured to be 814.8718E+18m³, while V_{BD} at B+ was positive indicating that the sample was P-Type. Moreover, the comparison between the values obtained automatically and manually had an error of 0.32% implying that the automated system is efficient.

5.0 Summary

Accurate Hall Effect measurements become more crucial as the requirement to characterize thin film semiconductor materials becomes more demanding. A simple, portable computer-aided Hall Effect measurement system for Hall Effect measurements has been designed and made. This system was able to control Keithley models 2182A, 6220, and 7001. A Germanium semiconductor thin film sample was fixed at a fabricated four-point probe and then put perpendicularly across an electromagnet. A LabVIEW-based VI and SubVIs were coded and compiled to create a simple program to collect, collate and analyze the electrical and electronic characterization of semiconductor samples using the Hall Effect method. The analysis was then exported as a report. The data obtained was validated by checking the consistency and repeatability which was affirmative.

6.0 Conclusion

The LabVIEW graphical software IDE provided a platform for creating an application package able to interface with Keithley models 2182A, 6220, and 7100 via the GPIB port. These devices were able to be set up and configured to enable them to communicate with the PC via the LabVIEW IDE. Additionally, LabVIEW VIs and SubVIs were coded for data analysis and PC presentation as well as data gathering from peripherals. A thin-film sample's resistance, resistivity, conductivity, Hall Coefficient, carrier mobility, Hall Angle, charge carrier concentration, and the type of doping have all been measured using a software-based approach.

The concentration of the charge carriers in my sample was 8.1487×10^{22} electrons per cubic meter and an R_H of $7.6595 \times 10^{-3} \Omega\text{m/T}$. The experimental values obtained had been determined to be consistent with the behavior of the measured carrier concentration. As reported by Nash [23], since the carrier capacity is connected to sample manufacturing and is dependent on the material used to make the germanium, there is no board to compare this to. However, the comparison between the automated generated data and the manually done experimental data had insignificant differences which strongly implies that the developed system is operating properly. From the measurements obtained, it is concluded that the automated system offers a simple, effective, and reliable method for thin film Hall Effect electrical characterization.

REFERENCES

1. Chen, N., *Semiconductor Thin Films for Information Technology*. Inorganic and Organic Thin Films: Fundamentals, Fabrication and Applications, 2021. **1**: p. pg 257-284.
2. Sarah, R. *Semiconductor Industry Association*. Global Semiconductor Sales, units shipped reach all-time highs in 2021 as industry ramps up production amid shortage 2022 Feb 14, [cited 2022 Apr 4]; Available from: <https://www.semiconductors.org/global-semiconductor-sales-units-shipped-reach-all-time-highs-in-2021-as-industry-ramps-up-production-amid-shortage/>.
3. Theis, T.N. and H.-S.P. Wong, *The end of moore's law: A new beginning for information technology*. Computing in science & engineering, 2017. **19**(2): p. 41-50.
4. Jamal, D.F., Pascal, *Electrical Characterization of Semiconductor Materials and Devices*. 2017. **20**(Springer Handbook of Electronic and Photonic Materials).
5. McCain, A., *How Fast Is Technology Advancing? [2022]: Growing, Evolving, And Accelerating At Exponential Rates – Zippia*. 2022.
6. Green, R., *Hall Effect Measurements in Materials Characterization | Tektronix*. 2011.
7. Wang, C.-R., et al., *Magnetotransport in copper-doped noncentrosymmetric BiTeI*. Physical Review B, 2013. **88**(8).
8. Onwujariri, T., *Significance of the Hall Effect On SemiConductors*. GulpMatrix, 2020.
9. Miccoli, I., et al., *The 100th anniversary of the four-point probe technique: the role of probe geometries in isotropic and anisotropic systems*. Journal of Physics: Condensed Matter, 2015. **27**(22).
10. Chien, C., *The Hall effect and its applications*. 2013: Springer Science & Business Media.
11. Schindler, L.A., et al., *Computer-based technology and student engagement: a critical review of the literature*. International journal of educational technology in higher education, 2017. **14**(1): p. pg 1-28.
12. Hauer, F., *Labforward & SpreadJS*. 2020.
13. Liscouski, J., *Computerized Systems in the Modern Laboratory: A Practical Guide*. 2015.
14. Coito, F.P., Luís Brito. *A remote laboratory environment for blended learning*. in *Proceedings of the 1st international conference on Pervasive Technologies Related to Assistive Environments*. 2008.
15. Agumba, J., et al., *Design and Fabrication of a simple four-point probe system for electrical characterization of thin films*. International Journal Of Current Research, 2011.
16. Cervantes, A.d.J.R., E.R. Gonzalez, and J.C. Alvarez. *Development and automation of a thermoelectric characterization system*. in *2018 International Conference on Mechatronics, Electronics and Automotive Engineering (ICMEAE)*. 2018. IEEE.
17. Garnica, B.S.A., K. Marius, and F. Sergej, *Automatic Micro-Robotic Identification and Electrical Characterization of Graphene*. Micromachines, 2019. **10**(12): p. pg 870.

<https://doi.org/10.53819/81018102t4208>

18. Valladares, S., et al., *Design and Implementation of an Automatic System for Dielectric Characterization of Ceramic Materials*. LACCEI, Inc., 2019.
19. Villarreal, R. and A. Ivón, *NI-VISA Write: basic exercises*. Virtual Instrumentation. Session 6. VISA R/W, 2022.
20. Bress, T. and B.A. Hamilton, *Effective LabVIEW Programming*. 2013.
21. Cai, W., B. Wang, and S. Zhang, *Remote Control and Data Acquisition of Multiple Oscilloscopes Using LabVIEW*, in *2017 International Conference on Computer Technology, Electronics and Communication (ICCTEC)*. 2017, IEEE. p. pg 920–924.
22. Yousif, H., *How to validate experimental data?* 2018.
23. Nash, S., *Characterizing Germanium with the Hall Effect*. Department of Physics, 2018(The College of Wooster, Wooster, Ohio 44691, USA).

APPENDIX

Manually vs Automatically collected data

I (A)	VBD B+ (V)		VDB B- (V)		VBD B- (V)		VDB B+ (V)	
	Manual	Auto	Manual	Auto	Manual	Auto	Manual	Auto
0	0	0	0	0	0	0	0	0
0.0005	0.00207	0.00199	-0.000069	-0.000068	-0.001997	-0.001939	0.000071	0.000072
0.001	0.003823	0.003901	-0.000141	-0.000138	-0.003768	-0.003806	0.000143	0.000146
0.0015	0.005943	0.005826	-0.00021	-0.000208	-0.005511	-0.005681	0.00022	0.00022
0.002	0.007984	0.007751	-0.000271	-0.000279	-0.007785	-0.007558	0.000286	0.000295
0.0025	0.00939	0.00968	-0.000339	-0.000349	-0.00915	-0.009433	0.000369	0.000369
0.003	0.011707	0.011591	-0.000435	-0.000418	-0.01097	-0.011309	0.000456	0.000443
0.0035	0.011707	0.011591	-0.000489	-0.000489	-0.01231	-0.01131	0.000537	0.000516
0.004	0.015595	0.015441	-0.00057	-0.000559	-0.014461	-0.015064	0.000598	0.000592
0.0045	0.018069	0.017374	-0.00063	-0.00063	-0.016949	-0.016949	0.000695	0.000668
0.005	0.018521	0.019293	-0.000671	-0.000699	-0.01806	-0.018812	0.000733	0.00074
0.0055	0.021857	0.02122	-0.000777	-0.000769	-0.020693	-0.020693	0.000793	0.000809
0.006	0.023608	0.023145	-0.000847	-0.000839	-0.023477	-0.022574	0.000876	0.000885
0.0065	0.026076	0.025073	-0.000874	-0.00091	-0.025437	-0.024459	0.000919	0.000957
0.007	0.026176	0.026986	-0.000919	-0.00098	-0.027423	-0.026368	0.000996	0.001027
0.0075	0.030075	0.028918	-0.001039	-0.001049	-0.027682	-0.028247	0.001043	0.001099
0.008	0.030843	0.030843	-0.001141	-0.001119	-0.030132	-0.030132	0.001146	0.001174
0.0085	0.03376	0.032777	-0.001226	-0.00119	-0.033307	-0.032026	0.001224	0.001244
0.009	0.034344	0.034691	-0.0013	-0.00126	-0.034572	-0.033894	0.001319	0.001319
0.0095	0.036985	0.036619	-0.001321	-0.001331	-0.036137	-0.035779	0.001346	0.001388
0.01	0.038163	0.038548	-0.001384	-0.0014	-0.037217	-0.037709	0.001401	0.001459
0.0105	0.040481	0.040481	-0.001498	-0.001469	-0.038802	-0.039594	0.001476	0.00153
0.011	0.042678	0.042406	-0.001538	-0.001538	-0.040144	-0.041485	0.001556	0.001597
0.0115	0.042987	0.044317	-0.001569	-0.001607	-0.042068	-0.043369	0.001596	0.001663
0.012	0.047178	0.046253	-0.001642	-0.001675	-0.043444	-0.045254	0.001678	0.00173
0.0125	0.04866	0.048178	-0.001745	-0.001745	-0.047151	-0.047151	0.001766	0.001794
0.013	0.050614	0.050111	-0.00176	-0.001814	-0.050019	-0.049038	0.001803	0.001878
0.0135	0.051502	0.052022	-0.001882	-0.001882	-0.052437	-0.05091	0.001924	0.001954
0.014	0.053424	0.053964	-0.001922	-0.001953	-0.052516	-0.052804	0.001975	0.002015
0.0145	0.056128	0.055892	-0.00198	-0.002021	-0.053547	-0.054736	0.002021	0.002084
0.015	0.057241	0.057819	-0.002132	-0.00209	-0.056927	-0.056626	0.002107	0.00215
0.0155	0.060327	0.05973	-0.002157	-0.002157	-0.059687	-0.058517	0.002225	0.002214
0.016	0.060427	0.06166	-0.002272	-0.002227	-0.06021	-0.060398	0.002303	0.002284
0.0165	0.061044	0.063588	-0.002294	-0.002294	-0.061673	-0.062296	0.002341	0.002352
0.017	0.063831	0.065521	-0.002405	-0.002364	-0.064295	-0.064195	0.002406	0.002427
0.0175	0.066088	0.067437	-0.002487	-0.00243	-0.065092	-0.066074	0.002525	0.002495
0.018	0.067977	0.069364	-0.002525	-0.0025	-0.067982	-0.067982	0.002564	0.002562

I (A)	VBD B+ (V)		VDB B- (V)		VBD B- (V)		VDB B+ (V)	
	Manual	Auto	Manual	Auto	Manual	Auto	Manual	Auto
0.0185	0.070439	0.0713	-0.002542	-0.002568	-0.071267	-0.06987	0.00258	0.002619
0.019	0.071767	0.073232	-0.002601	-0.002635	-0.072451	-0.071772	0.00266	0.002687
0.0195	0.075405	0.07515	-0.002666	-0.002698	-0.07446	-0.07366	0.002779	0.002754
0.02	0.077086	0.077086	-0.002765	-0.002765	-0.075533	-0.075555	0.002855	0.002811